Korean J. Chem. Eng., **30**(7), 1347-1358 (2013)
DOI: 10.1007/s11814-013-0101-0

INVITED REVIEW PAPER

Non-vacuum deposition of CIGS absorber films for low-cost thin film solar cells

Dongwook Lee and Kijung Yong†

Surface Chemistry Laboratory of Electronic Materials (SCHEMA), Department of Chemical Engineering, POSTECH, Pohang 790-784, Korea
(*Received 1 May 2013 • accepted 3 June 2013*)

Abstract−Thin film solar cells composed of chalcopyrite $Cu(In_{1-x}Ga_x)(Se_{1-y}S_y)_2$ (CIGSSe) absorbers have gained considerable attention in recent years in an effort to develop sustainable technologies for harnessing clean energy. Non-vacuum solution methods can reduce production costs by replacing vacuum-based deposition methods with large-scale, high-throughput processes. The efficient use of materials can reduce production costs. Non-vacuum processes generally rely on two sequential steps: solution-coating, followed by a post-annealing process. Depending on the point at which the CIGS phase evolves, non-vacuum processes can be categorized as nanoparticle (NP) approaches or molecular precursor approaches. These two types of liquid processes are believed to be compatible with a variety of applications, such as roll-to-roll coating for the production of flexible, portable devices. Additional thermal treatments using a gaseous chalcogen or oxygen can improve the absorber quality. This review describes the current status of chalcopyrite thin film solar cells fabrication methods via low-cost solution routes. An analysis of recently published reports describing liquid-based deposition methods is introduced, and the features of the development steps are compared. Finally, a discussion and future outlook are offered.

Key words: CIGS, Thin Film Solar Cell, Non-vacuum Process, Solution Deposition, Nanoparticle, Molecular Precursor

INTRODUCTION

In an effort to satisfy the continuously rising energy demands, a variety of alternative energy sources have been studied. Throughout most of the last century, solar energy was considered a promising candidate for clean and renewable energy source because it is economically feasible and does not produce harmful pollution during production. The recent global solar market can be classified into several photovoltaic technology types: silicon film-based solar cells, compound semiconductor thin film solar cells, dye-sensitized solar cells, and organic solar cells. Silicon-based photovoltaics have remained the solar cell material of choice; however, thicker and higher-quality silicon wafers, produced by intensive energy consuming process, should be required to allow enhanced charge transport and diffusion near a depleted junction [1,2].

Among the various solar cell designs, thin film solar cells that use inorganic compound semiconductor films as the absorbers are considered to be the most promising candidates for next-generation cells. Polycrystalline CIGS thin films have attracted both academic and industrial interest because they display a high optical absorption coefficient, tunable band gap energy, long-term chemical stability, and a high efficiency compared to other materials. With the high absorption coefficient of CIGS, over 90% of the incident photons can be absorbed in a thickness less than 2 μm. Over the past several years, CIGS thin film solar cells have broken the 20% of efficiency record and reduced the performance gap compared to silicon solar cells [3-5].

Most substrate-based CIGS solar cells are prepared with a typical configuration that includes several metals and semiconducting thin films, as shown in Fig. 1. The basic structure of the substrate configuration in a CIGS thin film solar cell includes a CIGS absorber/buffer p-n junction and highly conducting films on both sides of the p-n type semiconductor [3,4,6,7]. Low-cost, thermally stable soda-lime glass is the most commonly used substrate in CIGS solar cells because sodium diffusion from soda-lime glass improves the formation of a fine absorber grain structure [8,9]. RF or DC-sputtered molybdenum layers as back-contact electrodes are deposited on a substrate to take advantage of molybdenum's good electrical conductivity, long-term chemical/thermal inertness, and mechanical

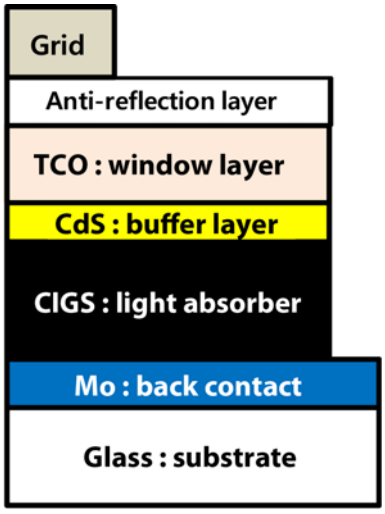

Fig. 1. Schematic diagram showing a conventional 'substrate'-type configuration for a CIGS thin film solar cell.

†To whom correspondence should be addressed.
E-mail: kyong@postech.ac.kr

properties [10-12]. A CIGS film is deposited as an absorber layer onto a Mo back contact, and photo-induced charge generation can occur via the absorption of incident solar light in this layer. A buffer layer that displays n-type conductivity and a wide band gap, such as CdS or ZnS, combined with a CIGS thin film to form p-n junctions [13,14]. To collect the photo-generated charges without optical loss prior to the arrival of incident light at the absorber, transparent conducting oxides (TCO) are the most common materials for the front contact layers [13]. Alloyed metal grids (Ni-Al) and anti-reflection layers (MgF_2) are usually used in high-performance photovoltaic devices.

The most important step in the fabrication of a CIGS thin film solar cell is the CIGS absorber deposition process because the deposition conditions determine the overall production cost and device performance. A wide variety of methods have been developed for the deposition of CIGS chalcopyrite thin films. Among the various approaches, particular thin film deposition techniques should be carefully implemented because of their interplay between the power conversion efficiency, cost, and reliability. Films with a suitable composition profile, phase purity, and fine grain structure are typically deposited using vacuum-based techniques, such as evaporation or sputtering [4,7,15,16]. Thermal evaporation or sputtering methods have been used to deposit a variety of precursors, such as elemental metals, chalcogens, or binary sources. The deposited raw materials are then converted into a CIGS phase through post-treatments. Deposition under highly evacuated environmental conditions and the application of a high-temperature post-treatment yield well-crystallized CIGS films that feature large grains, smooth surfaces, and a controllable composition profile without impurities. Recently, the 20% efficiency limit for CIGS solar cells was surpassed, and a champion cell efficiency of 20.4% was recorded by EMPA in Switzerland [17]. Four elements, Cu, In, Ga, and Se, were co-evaporated in a three-stage process to form a CIGS film that displayed a considerable performance enhancement. Although vacuum-based synthetic routes provide high-efficiency films, they cannot guarantee cost reductions in continuous mass production scaled-up processes with an efficient use of source materials because vacuum-based deposition techniques often require sophisticated deposition equipment and a high initial investment.

For these reasons, several inexpensive methods have been developed involving solution-based deposition approaches. This review highlights recent progress toward the development of non-vacuum thin film deposition approaches. We focus on two representative non-vacuum approaches involving nanoparticles or a molecular approach, describing the basic synthetic concepts, resulting device performances, and the strengths and weaknesses of each individual process. Finally, we offer a brief outlook on the fabrication of low-cost CIGS thin film solar cells.

NON-VACUUM PROCESSES FOR THE PREPARATION OF CIGS THIN FILM SOLAR CELL

Non-vacuum coating methods based on liquid processes are expected to facilitate the development of industrial-scale, fast, continuous roll-to-roll production methods that require a low initial capital cost. The demand for expensive materials, such as In and Ga, has gradually increased over the last few years in the electronic industry. Processes that make more efficient use of such materials could reduce the material costs and the generation of processing wastes to overcome the barriers to commercialization. Low-cost sequential deposition methods at low temperatures apply well-dispersed solutions containing CIGS nanoparticles or CIGS precursors, which are then dried or post-treated using chemical or thermal methods at higher temperatures. Schematic illustrations of two non-vacuum processing for preparing CIGS thin film solar cells are depicted in Fig. 2. Over the past few years, several challenging approaches

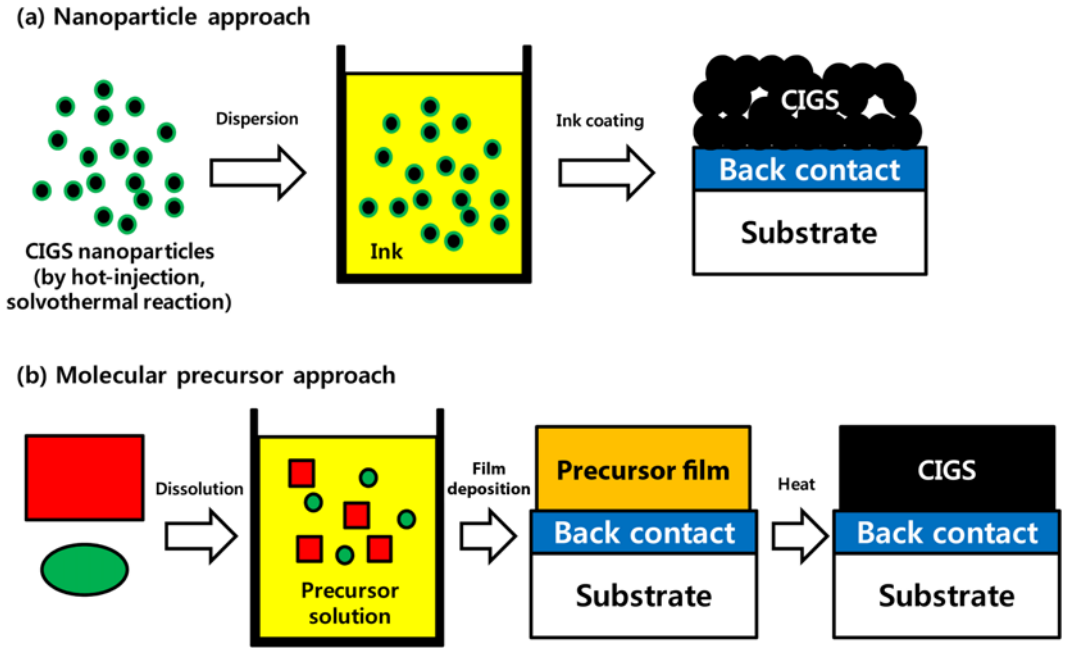

Fig. 2. Schematic diagram showing the synthetic processing steps involved in non-vacuum deposition approaches to preparing CIGS thin film solar cells: (a) nanoparticle approach and (b) molecular precursor approach.

have been tested for the low-cost deposition of CIGS layers. In this review, the various non-vacuum processing routes for depositing CIGS absorbers may be grouped into two main categories: nanoparticle or molecular precursor approaches.

1. Nanoparticle Approach

Nanoparticle (NP) approaches generally proceed through two steps: the synthesis of NPs and the ink deposition. The CIGS inks used for film deposition are usually prepared from CIGS NPs and a dispersion solvent. Numerous NP synthetic routes have been explored for implementing chalcopyrite thin film solar cells [18-37]. NPs (or quantum dots) are commonly synthesized using hot-injection or solvothermal reactions [36,38,39]. CIGS NPs may be rinsed and modified using ligand exchange techniques to improve dispersibility in certain nonpolar solvents, such as chloroform or toluene. The passivation of nanocrystal surfaces can prevent precipitation and ensure an ink's stability. After ink formation, CIGS inks are transferred onto a desired substrate using liquid deposition techniques (dip-coating, drop-casting, spray coating, etc.) under ambient condition. The CIGS phases are solidified and crystallized at elevated temperatures prior to deposition; therefore, the NP approach is compatible with flexible substrates, which are frequently sensitive to chemical and thermal degradation [40].

1-1. Synthesis of CIGS Nanoparticles

As shown in Fig. 3, hot-injection CIGS thin film approaches prepare CIGS nanocrystals via the rapid injection of cold reagents into a pre-heated reaction vessel containing organic surfactants, such as oleylamine, trioctylphosphine (TOP), trioctylphosphine oxide (TOPO), or other organic molecules that contain long carbon chains which passivate the surfaces of the nuclei [38,39]. The addition of reagents suddenly increases the precursor concentration above the nucleation threshold and results in the formation of uniform nanocrystals. The long carbon chain molecules slow down the growth of nuclei considerably by coordinating to the surfaces of the metal ions, thereby forming a steric barrier that prevents the approach of the reactants. These effects result in the synthesis of monodisperse, size-controlled NPs. Surface-modified NPs are readily dispersed in solvents to form stable colloids. The optical properties of nano-sized CIGS materials can be tuned according to the quantum confinement effects by varying the sizes and shapes of the NPs [41,42]; however, this approach requires the performance of complicated synthetic procedures under isolated argon atmospheres. NP synthesis approaches generally suffer from low yields and incur tedious purification steps.

Solvothermal reactions are extensively used to produce nanostructured inorganic materials through a chemical reaction in a closed system in which a solvent is brought to subcritical or supercritical conditions [43]. As shown in Fig. 4(a), these chemical reactions occur in sealed reaction vessels that enable the development of high-pressure and high-temperature conditions above the boiling point of the solvent to yield nano- or micro-sized inorganic materials. Solvothermal reactions require much simpler and milder conditions than hot-injection approaches; however, the as-prepared CIGS NPs display agglomerated morphologies (Fig. 4(b)-(d)) and non-uniform size distributions due to the non-uniform formation of nuclei upon heating the solution bath from room temperature [18-20]. Agglomerated CIGS NPs tend not to form stable NP inks because they form small-sized distributions.

1-2. CIGS Cell Performances Fabricated by Nanoparticle Approaches

Heat treatments induce the formation of interconnected nanocrystals. If heat treatments are not applied, the power conversion ef-

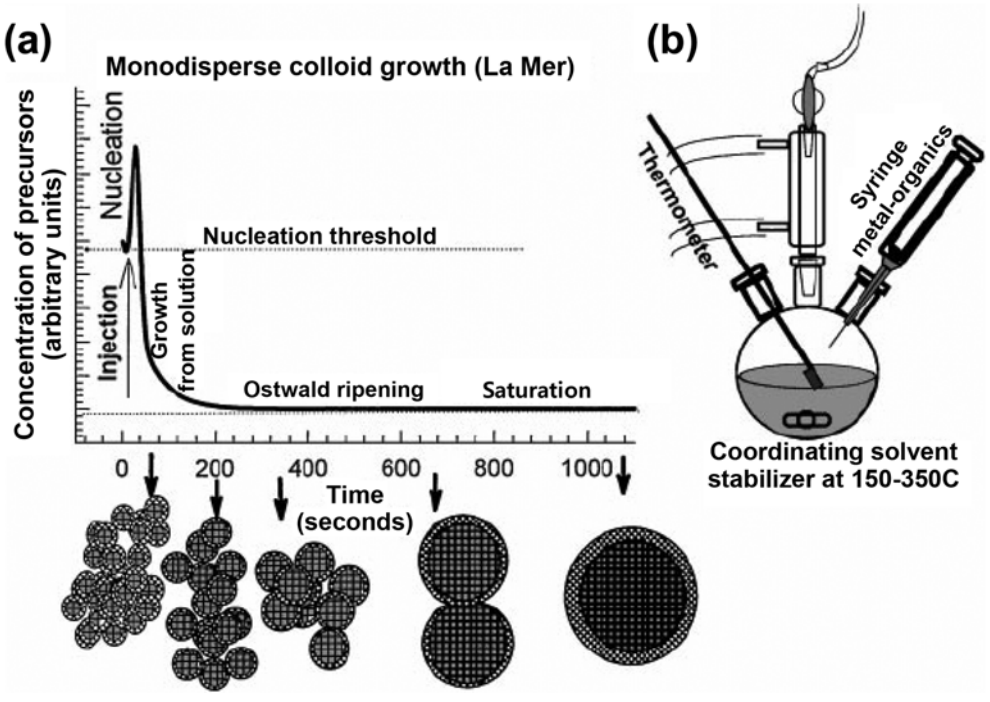

Fig. 3. (a) Schematic illustration depicting the stages of nucleation and growth for the preparation of monodisperse nanocrystals in the framework of the La Mer model. (b) Representation of the widely used simple synthetic apparatus employed in the preparation of monodisperse NC samples (from [39]).

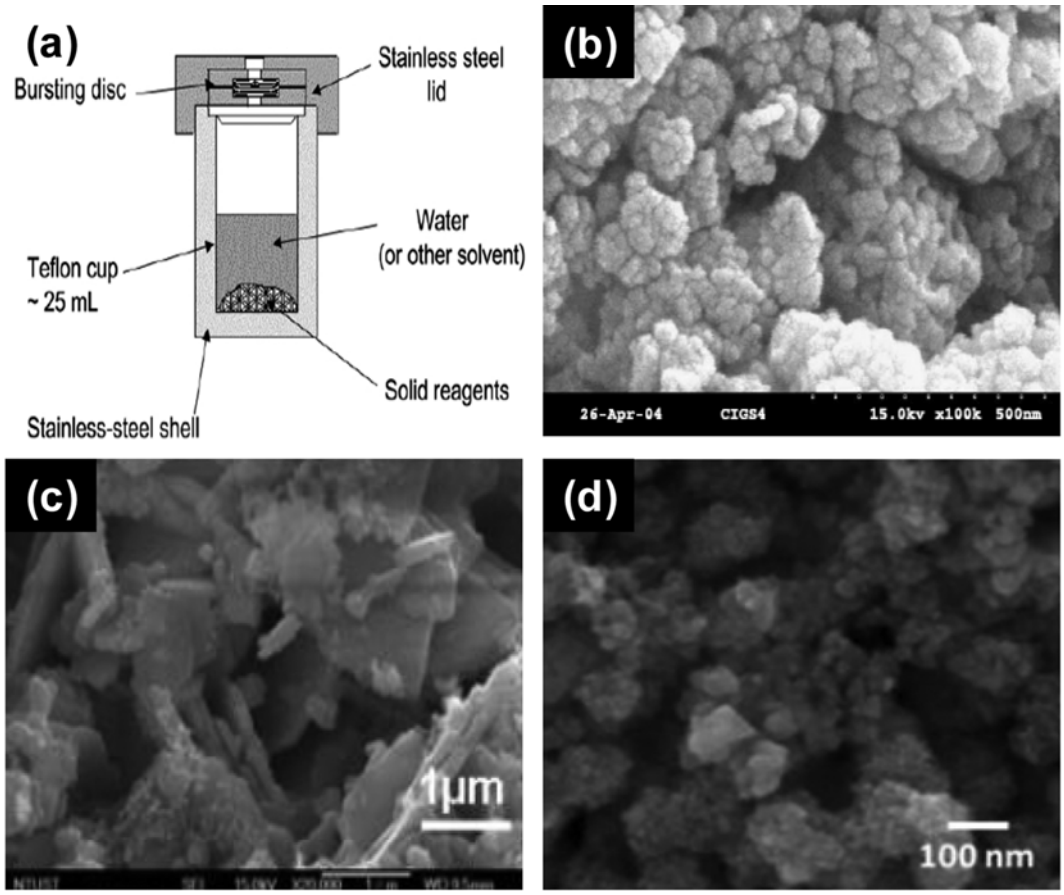

Fig. 4. (a) A schematic diagram of a stainless autoclave typically used in the laboratory to perform solvothermal synthesis (from [42]). Typical morphologies of the CIGS nanoparticles synthesized by solvothermal routes are shown in Fig. 4(b)-(d). Scanning electron microscopy (SEM) images of (b) CIGS nanoparticles obtained from the reactions at 230 ºC over 36 h using elemental metal and Se powder in ethylenediamine (from [31]); (c) CISe nanoparticles prepared by a microwave-assisted solvothermal method [19]; and (d) CIS nanocrystals prepared by a solvothermal reaction at 160 ºC over 12 h (from [20]).

ficiencies of the resulting ink-based CIGS thin film solar cells remain low. Panthani et al. demonstrated that drop-cast CIGS nanocrystal inks yielded a 0.24% efficiency [21]. They synthesized CIGS NPs with a diameter of 10 nm using hot-injection methods, as shown in Fig. 5(a)-(d). The film thickness could be controlled by varying the concentration of the nanocrystal inks (Fig. 5(e)). The final morphology of the as-casted absorber film resembled a pile of small nanocrystals. The low power conversion efficiency was attributed to a low short circuit current density (J_{sc}) and a low fill factor (FF). The high series and low shunt resistance arose from the poor nanocrystal quality. In 2010, the same research group reported a more optimized device configuration in which they tested the thickness-limited performance of a flexible CISe nanocrystal photovoltaic; however, as shown in Fig. 6, the power conversion efficiency of this device (3.1%) remained much lower than the efficiency obtained from vacuum-processed CIGS devices [44].

These examples illustrate the typical limitations of NP approaches. The performance of thin film photovoltaic devices is closely related to the grain structure and surface morphology of the absorber film. Low temperature, NP-based deposition processes do not provide a sufficiently high thermodynamic driving force to grow large crystallites with less grain boundaries. The grain boundaries act as recombination centers, reduce the efficiency of charge transfer in the absorber film, and generally yield a high series resistance [18]. Hindered charge transport and the reduced light absorption result from the long ligand chains required to achieve control over the NP sizes and shapes [45].

To overcome the low quality of ink-deposited CIGS films, Guo et al. suggested applying heat treatment to the nanocrystals [27]. Drop-casted films were sintered in a selenium-rich atmosphere to form large crystal domains that spanned the thickness of the film. In 2009, Guo et al. further reported that a selenization treatment of the $CuInS_2$ (CIS) nanocrystals reproducibly led to the full replacement of sulfur with selenium, which expanded the film volume and produced a densely sintered porous CIS absorber film [46]. Also, the introduction of high-temperature selenization processes compensated for the selenium loss at high temperatures and promoted the removal of surface passivation organic ligands.

The sintered CIGS NP films exhibited higher photovoltaic efficiencies than the as-deposited nano-CIGS films [23,47-49]. A dramatically enhanced efficiency (12%) was recently recorded by Hillhouse and Agrawal [49]. Sulfur-based CIGS NPs were selenized, and sodium doping was accomplished by soaking the film in a NaCl solution. Fig. 7 shows that the device performance improvement was mainly attributed to the formation of large and densely packed grains over the entire absorber layer thickness, obtained by the seleniza-

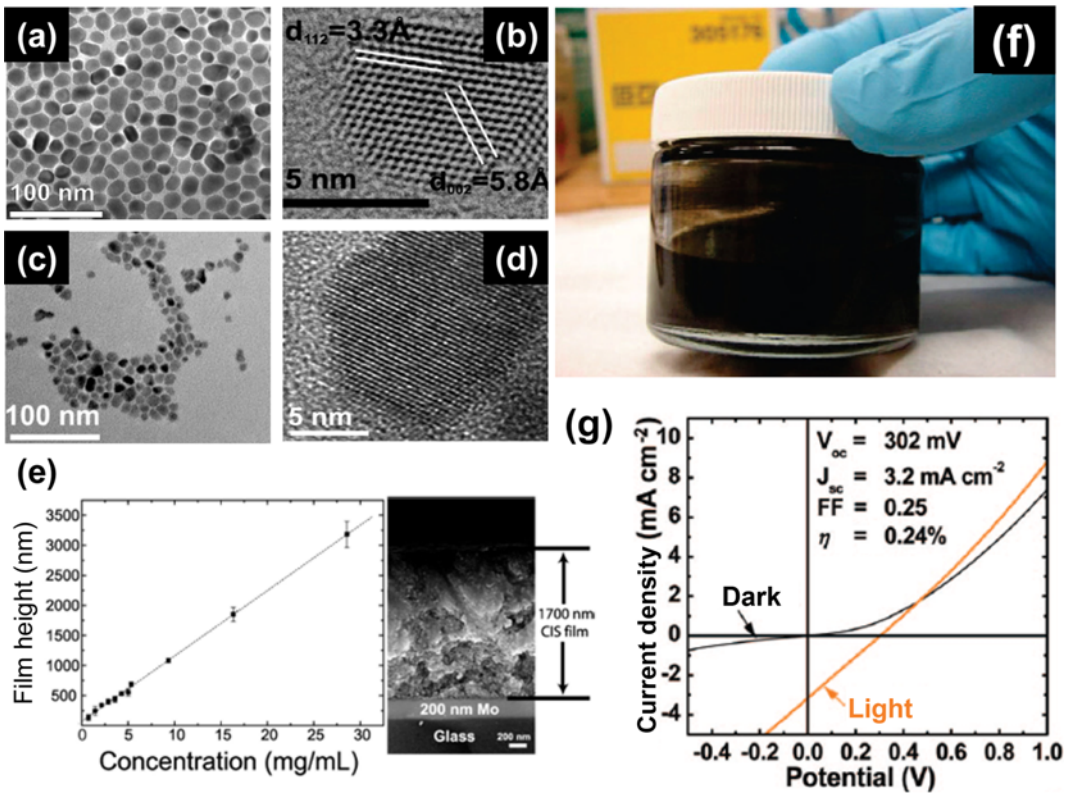

Fig. 5. Transmission electron microscopy (TEM) images of (a)-(b) $CuInSe_2$ and (c)-(d) $CuIn_{1-x}Ga_xSe_2$ nanoparticles synthesized by arrested precipitation in solution using organic surfactants (from [21]) (e). (Left) Thickness-controllable drop-casted film produced by varying the nanocrystal concentrations. (Right) SEM image of a drop-cast chalcopyrite film, showing small individual crystallites. (f) Digital image of a printable ink made of $CuInSe_2$ nanocrystals and non-polar solvents. (g) Dark and illuminated current density-voltage photovoltaic performances of an ink-deposited CISe device, yielding an efficiency of 0.24%, with J_{sc}=3.2 mA/cm^2, V_{oc}=302 mV and FF=0.25.

tion and NaCl treatment of the nanocrystal films. The presence of additional Na atoms played an important role in improving the structural properties of the CIGS films. Na-doping is well-known to enhance the (112)-oriented crystal structure of the vacuum-deposited CIGS thin film. However, to the best of our knowledge, Na-doping to grow bigger crystallites is unusual in NP-processed CIGS thin film [50-52]. Reduced recombination loss at the grain boundaries enhanced the device performance, particularly the open circuit voltage (V_{oc}) and FF.

A variety of synthetic methods have displayed potential utility for the preparation of low-cost thin film solar cells. Although an efficiency exceeding only 10% has been achieved using NP deposition methods followed by selenization, NP-based approaches represent a considerable step forward toward the practical manufacture of solar cells on flexible substrates, such as plastic films, which generally display melting or glass transition behaviors at the selenization temperatures (400-600 °C). Much simpler synthetic methods with better NP yields must be developed.

2. Molecular Precursor Approach

Molecular precursor methods involve the application of two sequential steps: the formation of a homogeneous precursor solution, which is then deposited, followed by application of an appropriate thermal treatment. A molecular precursor method was used to form a chalcopyrite phase directly on a substrate. This method is based on the direct coating of a solution containing a homogeneously dissolved metal precursor (Cu, In, Ga organics, salts, chalcogenides, etc.) and a chalcogen precursor in an organic solvent. The components of a molecular precursor solution are typically solvents, precursors, and additives. In many cases, the solvent is the most critical component because the choice of solvent determines whether the metal precursor is stabilized in solution at room temperature for long periods of time. Many factors are considered in the selection of an optimal solvent, including the boiling point, vapor pressure, polarity, surface tension, reactivity, toxicity, and cost. Organic solvents with a low boiling point (>300 °C), such as alcohols or amines, are universally used as solvents because they are relatively easy to handle without the need for protection or ventilation [53-64]. Metal precursors, such as metal halides, oxides, hydroxides, organics, or chalcogenides, are often used. The precursor-containing solutions can occasionally include chalcogen precursors (Se, S) [53-55,65-68]. The stoichiometry of the precursor solution is reflected in the film composition by controlling the molar ratio between the precursors. After the formation of a stable solution containing the constituent elements of the CIGS, the solution is transferred onto the surface of a substrate by using an appropriate coating technique, such as doctor-blade coating, spin-coating or ink rolling. Subsequent annealing eliminates the non-CIGS constituents, such as the solvents, additives, or by-products and converts the precursors to a chalcopyrite phase. The most important factor is not the selection of the coating technique, but rather the ability of the as-deposited materials to form

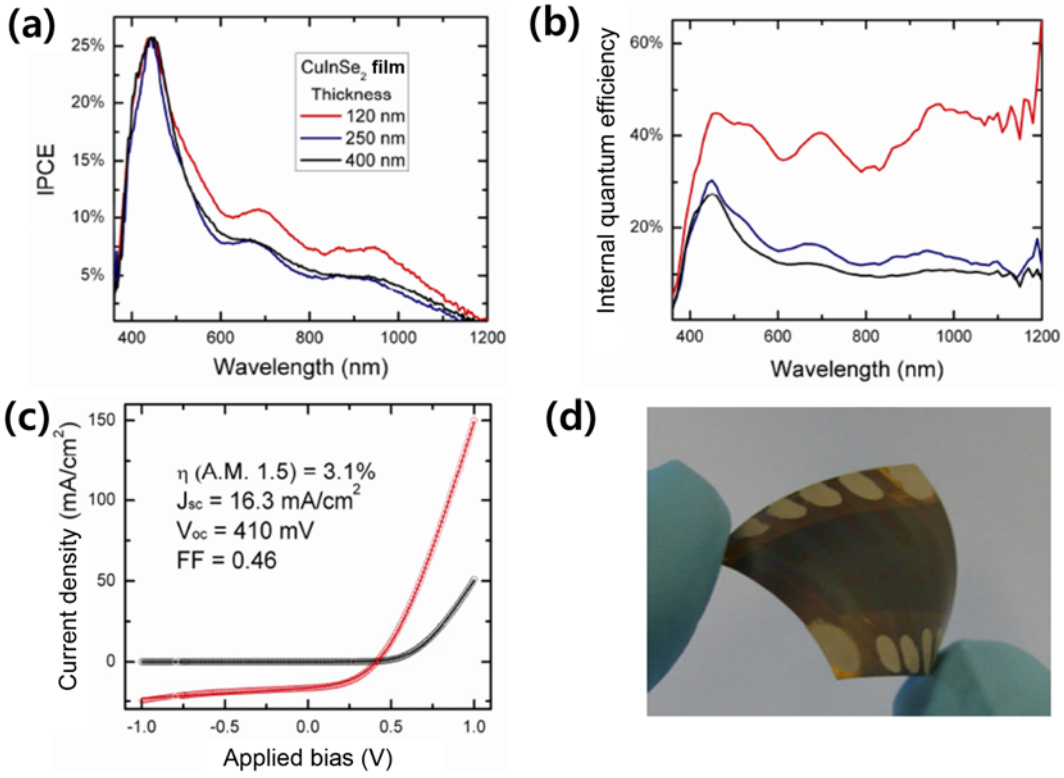

Fig. 6. (a), (b) The incident photon-to-electron conversion efficiency (IPCE), internal quantum efficiency (IQE), and the results of the CISe devices prepared with varying thickness values. The thinner devices displayed much better IPCE and IQE values, indicating that they efficiently extracted the photogenerated charge carriers across a wide range of wavelengths. (c) Current density-voltage characteristic of a device, showing a power conversion efficiency exceeding 3% using an absorber thickness of 120 nm. (d) Digital photograph of a flexible solar cell fabricated by spraying CIGS ink onto a plastic substrate (from [44]).

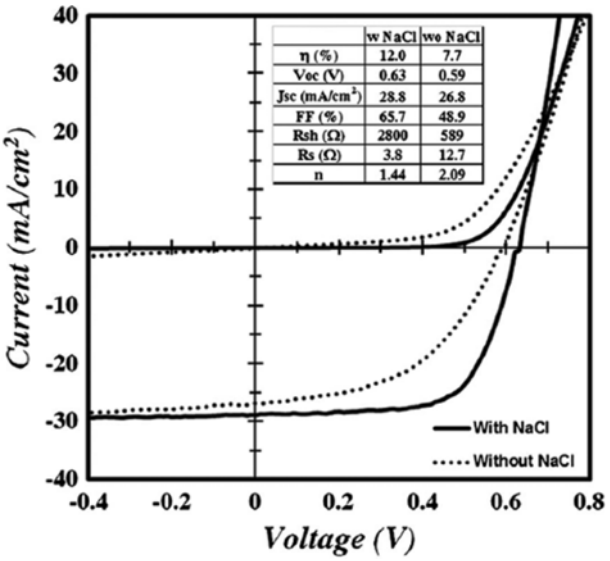

Fig. 7. Current density-voltage characteristics of the CIGSe thin film solar cells prepared with or without NaCl soaking, fabricated using nanoparticle deposition methods and selenization for nanocrystallite sintering (from [46]).

a high-quality final absorber film without voids, cracks, segregated domains, undesired binary phases, or other defects, upon drying and thermal or chemical treatment.

2-1. Hydrazine-based Precursor Solution Processes

Since the first report of a hydrazine-processed CIGS solar cell in 2008, hydrazine-based precursor solutions have been the most successful routes to achieving high-quality high-efficiency CIGS thin films using solution-based approaches. Mitzi et al. from IBM reported the development of hydrazine-based methods in 2004 for the preparation of high-mobility thin film devices [69]. They demonstrated a novel technique for preparing semiconducting tin disulfide (SnS_2) thin films by spin-coating a precursor dissolved in hydrazine. This molecular precursor method was then applied to the fabrication of solution-processed CIGS thin film solar cells. This approach was based on the concept of 'dimensional reduction', in which an excess of chalcogen (S or Se) is thought to improve the solubility of the metal chalcogenides in hydrazine [6]. A schematic diagram illustrating the concept of 'dimensional reduction' is provided in Fig. 8(a). Metal chalcogenides have a limited solubility in most conventional organic solvents, such as alcohols or amines, at room temperature; however, the presence of excess chalcogens in the hydrazine solution disrupts the metal chalcogenide framework to form soluble anionic species separated by small volatile cationic species. Highly soluble and stable hydrazinium-based metal chalcogenides precursors then form continuous and uniform semiconducting films through the thermal decomposition of the starting metal precursors at an appropriate temperature. Hydrazine is an organic solvent containing two amine groups and is sufficiently volatile that it is removed from the as-deposited precursor film under heat treatment.

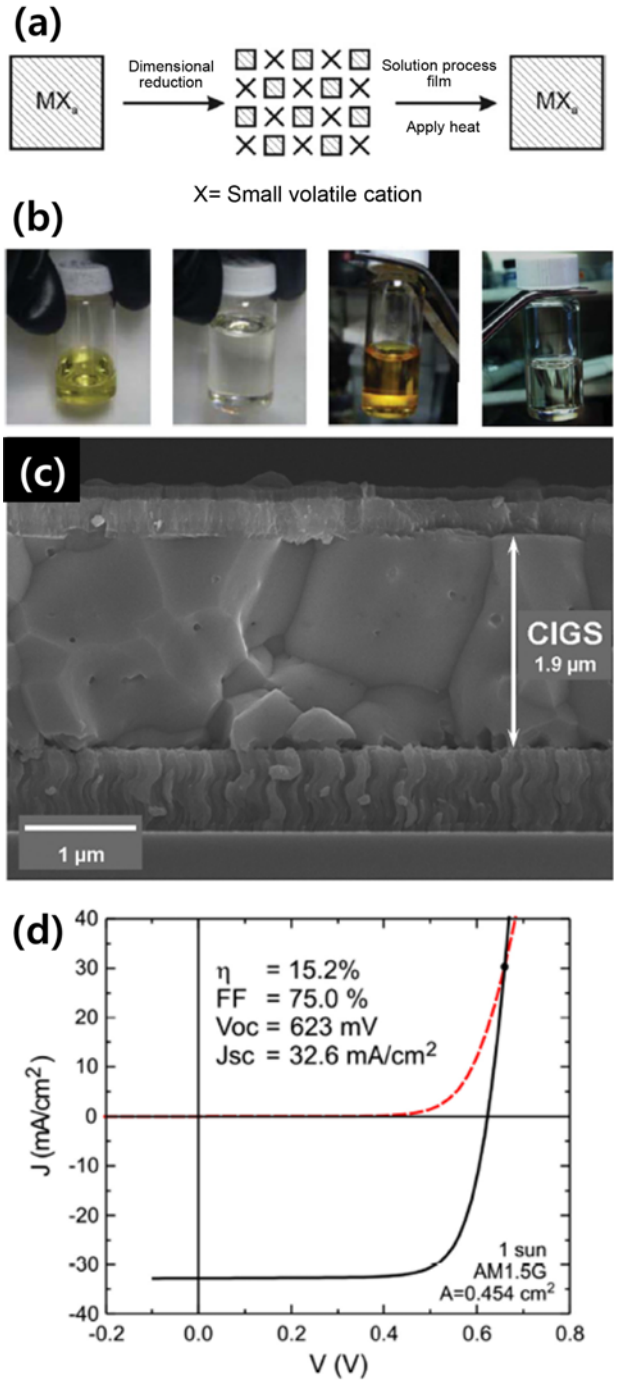

Fig. 8. (a) Schematic diagram illustrating the hydrazine-based molecular precursor approach based on the concept of 'dimensional reduction'. The presence of excess chalcogens induced the dissociation of smaller hydrazine-soluble ionic species from the bulk metal chalcogenide (from [6]). (b) Photographs of (from left to right) Cu_2S, In_2Se_3, mixed $CuInSe_2$, and Ga dissolved in hydrazine (from [70]). (c) Cross-sectional SEM image of a hydrazine-processed CIGS device structure (Mo/CIGS/CdS/ZnO/ITO/Ni-Al). (d) Current density-voltage characteristics of a hydrazine-processed device under illuminated conditions or dark conditions. A maximum efficiency of 15.2% was recorded based on a hydrazine molecular precursor approach in 2013. This approach reduced the performance gap between the solution-processed solar cells and the vacuum-deposited solar cells (from [68]).

Hydrazine does not include any carbon or oxygen atoms; therefore, it does not leave residual carbon contaminants in the high-quality inorganic semiconductor films.

A highly efficient solution-deposited CIGS photovoltaic cell was developed by Mitzi and coworkers using a hydrazine-based molecular precursor method (Fig. 8(b)-(d)) [65,70]. A chalcogenide precursor solution (containing Cu_2S, In_2Se_3, Ga_2Se_3, S, and Se) in a hydrazine solvent was repeatedly spin-coated (Fig. 8(b)) and subsequently annealed under an inert atmosphere (400-525 °C) until the desired absorber thickness was achieved. The deposited CIGS films showed no carbon or oxygen contamination at the detection limit of Auger analysis. The best cell, prepared over a laboratory-scale device area, yielded a total area power conversion efficiency of 10.3%. The latest report from this research group described the optimized procedure for the preparation and deposition of a hydrazine-based solution, which yielded a CIGS thin film solar cell that reached a new efficiency record [68]. A power conversion efficiency of 15.2%, along with a J_{sc}=32.6 mA/cm^2, V_{oc}=623 mV, and FF=75%, is the highest value yet achieved for a CIGS thin film solar cell fabricated purely using solution-based approaches. Even the defects were broadly

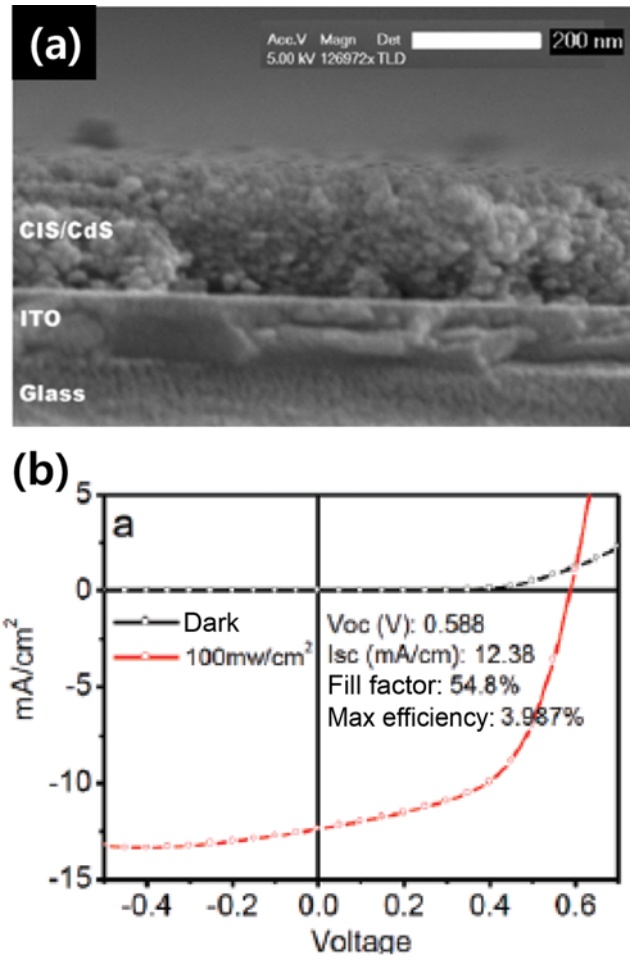

Fig. 9. (a) SEM image of the CIS film prepared via an in-situ synthesis and deposition method using a sulfur precursor-containing molecular precursor solution, followed by heat treatment under mild conditions. (b) The photovoltaic performance of a corresponding ITO/CIS/CdS/Al device yielded an efficiency of 3.987% (from [6]).

distributed, the minority carrier life time was low, and the series resistance was high, J_{sc} and FF yielded comparable values to those achieved from a vacuum-processed cell with a similar band gap (~1.1 eV) [5]. However, hydrazine poses several safety and environmental concerns; therefore, replacement solvents must be found, even though hydrazine methods yield the highest photon conversion efficiencies. In addition, the deposition and heat treatment processes must be handled under an inert atmosphere to prevent the incorporation of oxygen.

2-2. Non-hydrazine-based Precursor Solution Processes

The limitations on the use of hydrazine have led many research groups to seek safer and simpler molecular precursor methods that rely on low-toxicity solutions. One such method involves a non-toxic solution-processed photovoltaic device prepared with chalcogen precursors. This method is expected to eliminate the need for additional processing steps for applying the chalcogen, such as selenization or sulfurization. Thiourea ($CS(NH_2)_2$) and thioacetamide ($CSNH_2CH_3$) are the most widely used chalcogen precursors for solution-processed semiconducting materials [71]. Unfortunately, these organic chalcogen precursors react easily with metal cations at room temperature to produce undesirable precipitates.

Li et al. suggested a facile synthetic method that utilized significantly less toxic solvents [55]. 1-Butylamine and 1-propionic acid, which have boiling points below 230 °C, were used as the solvent and reaction stabilizer, respectively, to prevent the formation of precipitates [72]. Fig. 9 shows that spin-coating, followed by a drying process at moderate temperatures (250 °C) produced the in-situ formation of particle-like CIS thin films that displayed photovoltaic behavior with a J_{sc}=12.38 mA/cm^2, V_{oc}=588 mV, FF=54.8%, and an efficiency of 3.987%. This synthetic route is environmentally friendly and can be integrated into flexible polymer substrate processing involving, for example, polyimide substrates, due to the need for a low processing temperature.

Other non-vacuum processing routes that rely on non-hydrazine solvents have been developed and yield remarkable performance [56-64]. Many reports indicate that solution-processed CIGS thin film devices suffer from undesired residual impurities. Additives, and specifically the binders used to stabilize the solution and modulate the viscosity, are major sources of impurities. Fig. 10 shows that the use of a binder material often leads to the formation of a residual carbon layer between the Mo back contact layer and the CIGS absorber layer [53,54,56,59,63,73]. Polymeric binding materials generally enhance the viscosity, which reduces the number of coating cycles required to guarantee a flat uniform morphology. The influence of the carbon layer resulting from the organics in the precursor solution remains a controversial issue in CIGS thin film solar cells. The presence of a residual carbon layer is reported to play either a beneficial or a detrimental role in the performance of paste-coated CIGS thin film solar cells [56,59,74]. This factor must be considered during subsequent processing steps, as incomplete elimination can severely deteriorate the electronic properties or at least impede grain growth.

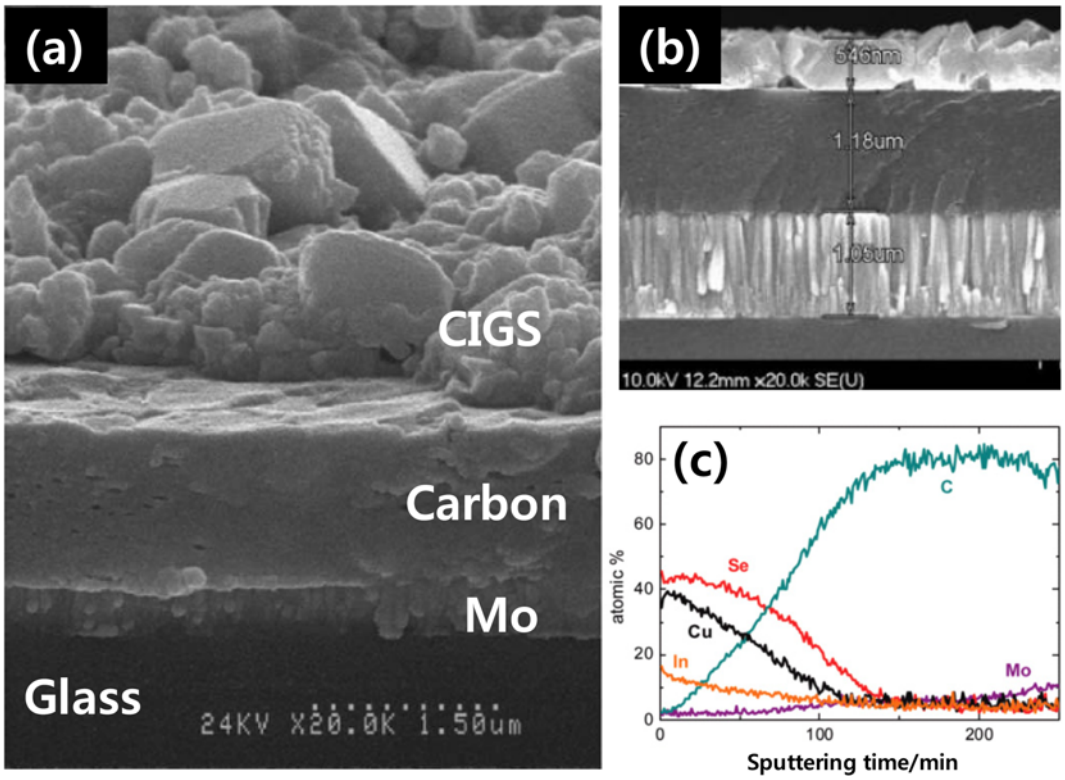

Fig. 10. Images of a typical double-layered structure produced using an organic binder. After the application of high-temperature heat treatments, such as selenization, a thick, dense, and well-crystallized upper CIGS layer developed and the polymeric organic binder remained under the CIGS layer as a carbonized residual layer. (a), (b) SEM images and (c) Auger electron spectroscopy (AES) reported previously. These results indicated the formation of a thick carbon layer between the absorber and metal electrode layers (from [56,73]).

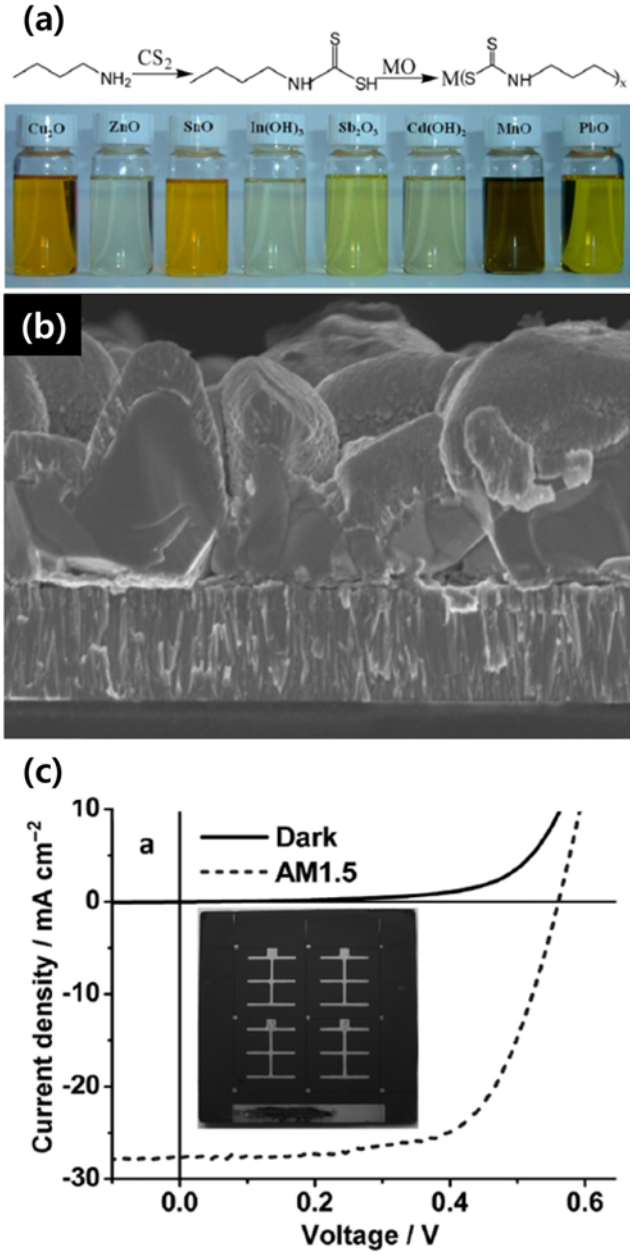

Fig. 11. (a) Formation mechanism in the presence of butyldithocarbamic acid, and a digital photograph of the various metal precursor solutions that displayed long-term stability. These solutions were compatible with the non-vacuum liquid-processing methods developed by Wang et al. (from [61]). (b) Cross-sectional view of the complete CIGSSe thin film photovoltaic device prepared by the selenization of an as-deposited precursor solution. (c) Measured photovoltaic performance of the Mo/CISSe/CdS/ZnO/ITO/Al structure, yielding a power conversion efficiency of 10.1% (from [64]).

Viscous precursor pastes are useful for rapidly preparing uniform coatings on a desired substrate. Precursor paste-based approaches have been described by Kaelin et al. using Cu, In, and Ga salts [56]. Absorbers were grown via doctor-blade coating and subsequent selenization of an as-deposited precursor film, yielding a double-layer structure with a CIGS absorber on top of an amorphous carbon layer (Fig. 10(a), (b)). Diffusion from the metal precursor to react with the vaporized selenium produced two separated phases on the Mo-coated substrate and a thick carbon layer segregated under the absorber layer. The photovoltaic properties reached a maximum efficiency of 6.7%, even with the formation of an amorphous carbon layer with thickness of several hundreds of nanometers.

To date, most efforts to reduce residual contaminants have attempted to apply additional oxidation prior to high-temperature annealing [57,58,62,63]. Carbon-free CIGS absorbers may be prepared by baking vulcanized or sticky paste-coated films in air to burn off the organics. The resulting air-stable mixed metal oxide films could then be converted into chalcopyrite phases through reaction with evaporated sulfur or H_2S gas at high temperatures. Carbon was not detected in the film after the air-heating and sulfurization processes. The resulting CIGS thin film with a smooth morphology was nearly free from carbon impurities and displayed a high conversion efficiency of 8.28% [63]. Uniform grain growth throughout the entire absorber film was achieved by applying high-pressure chalcogen vapor (H_2S, Se, S vapor, etc.). The effects of the complicated multi-step post-treatments were compared with the effects of the one-step annealing treatment. This synthetic method still poses several challenges as an alternative liquid-based process for the production of highly efficient thin film photovoltaics.

In an effort to exclude the complicated multi-step annealing process, a Chinese research group recently suggested a versatile strategy for synthesizing CIGS thin films through spin-coating of a molecular precursor solution without the use of organic binders [61]. Metal oxide or hydroxide precursors that were either stable or insoluble in conventional organic solvents could be readily dissolved in butyldithiocarbamic acid to form a thermally degradable metal-organic molecular precursor solution, as shown in Fig. 11(a). The prepared precursors were stable for at least six months in air and were highly soluble in common organic solvents. Devices were produced by spin-coating this solution, followed by selenization at 540 °C. These devices yielded a conversion efficiency as high as 10.1%, which approached the efficiencies achieved from hydrazine-processed solar cells. This synthetic method appears to be very useful for the fabrication of other liquid-processed semiconducting films, such as SnS or $Cu_2ZnSn(SeS)_4$ (CZTS), because a variety of metal-organic precursors may be readily stabilized in any solvent using this method.

SUMMARY & OUTLOOK

Table 1 summarizes the recent methodologies and photovoltaic performance of non-vacuum-processed CIGS thin film devices fabricated using nanoparticle approaches or molecular precursor approaches. Solution-processed CIGS thin film solar cells prepared using as-deposited nanoparticles displayed cell efficiencies of 0.24%, and the films prepared using hydrazine methods displayed cell efficiencies of 15.2%. Most solution-processed CIGS thin film solar cells fabricated at low temperatures may potentially be used with flexible substrates; however, their power conversion efficiencies have not yet reached levels sufficient for commercialization. The film qualities are low compared to the qualities obtained from vacuum-processed cells. Above all, these cells display poor V_{oc} and FF values due to the large number of grain boundaries and the presence of residual organic materials, both of which introduce recombination centers. Harsh chemical and thermal treatments may be applied after the

Table 1. Current status of photovoltaic performance of CIGS thin film solar cells fabricated via non-vacuum routes

Year	Absorber material	Coating method	Heat treatment	J_{sc} (mA/cm^2)	V_{oc} (mV)	FF	Efficiency (%)	Ref.
Nanoparticle approach								
Film deposition without additional heat treatment								
2008	CIS	Drop-casting	Drying in ambient condition	3.2	302	0.25	0.24	[21]
2010	CISe	Spray	Drying in ambient condition	16.3	410	0.46	3.1	[44]
Film deposition with additional heat treatment (selenization, RTA, etc.)								
2008	CIS	Drop-casting	Selenization (450-550 ºC)	25.8	280	0.39	2.82	[27]
2009	CIGSSe	Drop-casting	Sulfurization (500 ºC)	23.7	455	0.515	5.5	[46]
2012	CISe	Ink-casting	Selenization (530 ºC)	33.7	440	0.55	8.2	[48]
2012	CIGSSe	Doctor-blading	Selenization (500 ºC)	28.8	630	0.657	12.0	[49]
Molecular precursor approach								
Hydrazine-based molecular precursor solution								
2008	CIGSSe	Spin-coating	Annealing with inert gas (400-525 ºC)	25.7	605	0.66	10.3	[65]
2012	CIGSSe	Spin-coating	Annealing with inert gas (540 ºC)	32.6	623	0.75	15.2	[68]
Non-hydrazine-based molecular precursor solution								
Deposition followed by simple annealing in low temperature								
2009	CIS	Spin-coating	Air annealing (250-300 ºC)	12.38	588	0.548	3.987	[55]
Deposition followed by additional heat treatment (oxidation, selenization, sulfurization)								
2005	CIGSe	Doctor-blading	Selenization (560 ºC)	27.2	404	0.61	6.7	[56]
2010	CIS	Ink-rolling	Oxidation (370 ºC), Sulfurization (525 ºC)	18.49	320	0.37	2.15	[57]
2011	CIGSe	Ink-printing	Oxidation (300 ºC), Selenization (500 ºC)	29.78	386	0.44	5.04	[58]
2012	CISe	Spin-coating	Selenization (520 ºC)	36.393	420	0.505	7.72	[59]
2012	CIGSe	Knife-coating	Selenization (600 ºC)	31.8	419	0.58	7.7	[60]
2012	CIGSe	Spin-coating	Oxidation (350 ºC), Selenization (500-530 ºC)	25.69	525	0.59	8.01	[62]
2013	CIGS	Spin-coating	Oxidation (300 ºC), Sulfurization (500 ºC)	17.0	787	0.619	8.28	[63]
2013	CIGS	Spin-coating	Selenization (540 ºC)	27.64	561	0.65	10.1	[64]

coating of nanoparticle inks or precursor solutions to remove most of the non-CIGS impurities. The resulting devices generally perform better than the untreated devices. The record for the maximum device efficiency obtained from solution-processes CIGS thin film solar cells has been continuously broken by preparing films using hydrazinium precursors. The efforts of many research groups have steadily decreased the efficiency gap between CIGS thin film solar cells prepared by non-vacuum or vacuum-based synthetic methods.

This comprehensive review has described the state of the art for preparing low-cost CIGS absorber films, along with several recent approaches within the two main categories of synthetic preparation routes based on non-vacuum approaches. Vacuum-processed CIGS thin film solar cells are limited in their commercial potential by the costs and technological barriers. Recent developments in non-vacuum deposition processes are expected to enable the large-scale large-area production of low-cost solar modules in a high-throughput with a high material use efficiency. The best solar cell performance via liquid-based approach, achieved using a laboratory-scale active area, has yielded an efficiency of 15%. This value is considerably closer to the efficiency values for CIGS solar cells fabricated with co-evaporation methods. Also, deposition processes conducted at low temperatures show promise for achieving lightweight mechanically flexible and portable power production devices.

The basic properties of precursor solutions must be optimized to improve the solution stability against exposure to air at room temperature. Additional improvements must be made in the toxicities of the solutions and processes, the adhesion to the substrate, and the coating uniformity. Photovoltaic devices that lack impurities, voids, or cracks in the absorber film, which affect the device performance, are needed to improve the charge transport properties and collection efficiency while reducing the optical and recombination losses at the absorber layer. Post-deposition processes must be developed to facilitate grain growth and to sinter the separated nanocrystallites. These processes would be preferably conducted under milder conditions than those reported recently. Also, combining the advantages of the nanostructured ZnO or CdS with liquid-based deposition process can be a good solution to achieve better performance because more efficient charge separation and transfer are enabled due to the shorter traveling distance to the junction in nanostructured solar cell. Recently, well-aligned metal oxide nanostructures have been widely investigated as conductive channels, ensuring rapid collection of carriers generated at light absorbing materials [72,75-82]. Finally, a deeper understanding of the underlying physical and chemical mechanisms of the precursor decomposition, film formation, and densification processes could suggest future directions of research. With a comprehensive consideration of the fac-

tors that contribute to device performance, we predict a bright future for the development of non-vacuum processes for preparing CIGS thin film solar cells.

ACKNOWLEDGEMENT

This research was supported by the Converging Research Center Program through the Ministry of Education, Science and Technology (2012K001273) and NRF Research Fund (2013R1A2A2A05005344).

REFERENCES

1. A. F. Sherwani and J. A. Usmani, *Varun Renewable and Sustainable Energy Reviews*, **14**, 540 (2010).
2. A. V. Shah, H. Schade, M. Vanecek, J. Meier, E. Vallat-Sauvain, N. Wyrsch, U. Kroll, C. Droz and J. Bailat, *Progress in Photovoltaics: Research and Applications*, **12**, 113 (2004).
3. A. Romeo, A. Terheggen, D. Abou-Ras, D. L. Batzner, F. J. Haug, M. Kalin, D. Rudmann and A. N. Tiwari, *Prog. Photovoltaics*, **12**, 93 (2004).
4. S. Niki, M. Contreras, I. Repins, M. Powalla, K. Kushiya, S. Ishizuka and K. Matsubara, *Prog. Photovoltaics*, **18**, 453 (2010).
5. P. Jackson, D. Hariskos, E. Lotter, S. Paetel, R. Wuerz, R. Menner, W. Wischmann and M. Powalla, *Prog. Photovoltaics*, **19**, 894 (2011).
6. T. Todorov and D. B. Mitzi, *Eur. J. Inorg. Chem.*, 17 (2010).
7. U. P. Singh and S. P. Patra, *Int. J. Photoenergy*, **2010**, 19 (2010).
8. K. Sakurai, A. Yamada, P. Fons, K. Matsubara, T. Kojima, S. Niki, T. Baba, N. Tsuchimochi, Y. Kimura and H. Nakanishi, *J. Phys. Chem. Solids*, **64**, 1877 (2003).
9. J. H. Scofield, S. Asher, D. Albin, J. Tuttle, M. Contreras, D. Niles, R. Reedy, A. Tennant and R. Noufi, In Photovoltaic Energy Conversion, **1**, 164 (1994).
10. J. H. Scofield, A. Duda, D. Albin, B. L. Ballard and P. K. Predecki, *Thin Solid Films*, **260**, 26 (1995).
11. A. A. Kadam, N. G. Dhere, P. Holloway and E. Law, *J. Vac. Sci. Technol. A*, **23**, 1197 (2005).
12. H. Khatri and S. Marsillac, *J. Phys-Condens Mat.*, **20** (2008).
13. N. Naghavi, D. Abou-Ras, N. Allsop, N. Barreau, S. Bucheler, A. Ennaoui, C. H. Fischer, C. Guillen, D. Hariskos, J. Herrero, R. Klenk, K. Kushiya, D. Lincot, R. Menner, T. Nakada, C. Platzer-Bjorkman, S. Spiering, A. N. Tiwari and T. Torndahl, *Prog. Photovoltaics*, **18**, 411 (2010).
14. D. Hariskos, S. Spiering and M. Powalla, *Thin Solid Films*, **480**, 99 (2005).
15. P. Jackson, D. Hariskos, E. Lotter, S. Paetel, R. Wuerz, R. Menner, W. Wischmann and M. Powalla, *Progress in Photovoltaics: Research and Applications*, **19**, 894 (2011).
16. R. Klenk, J. Klaer, R. Scheer, M. C. Lux-Steiner, I. Luck, N. Meyer and U. Rühle, *Thin Solid Films*, **480-481**, 509 (2005).
17. *Optik & Photonik*, **8**, 4 (2013).
18. S. Yoon, T. Yoon, K. S. Lee, S. Yoon, J. M. Ha and S. Choe, *Sol. Energy Mater. Sol. C*, **93**, 783 (2009).
19. C. C. Wu, C. Y. Shiau, D. W. Ayele, W. N. Su, M. Y. Cheng, C. Y. Chiu and B. J. Hwang, *Chem. Mater.*, **22**, 4185 (2010).
20. W. C. Huang, C. H. Tseng, S. H. Chang, H. Y. Tuan, C. C. Chiang, L. M. Lyu and M. H. Huang, *Langmuir*, **28**, 8496 (2012).
21. M. G. Panthani, V. Akhavan, B. Goodfellow, J. P. Schmidtke, L. Dunn, A. Dodabalapur, P. F. Barbara and B. A. Korgel, *J. American Chem. Soc.*, **130**, 16770 (2008).
22. M. Y. Chiang, S. H. Chang, C. Y. Chen, F. W. Yuan and H. Y. Tuan, *J. Phys. Chem. C*, **115**, 1592 (2011).
23. J. H. Lee, J. Chang, J. H. Cha, Y. Lee, J. E. Han, D. Y. Jung, E. C. Choi and B. Hong, *Eur. J. Inorg. Chem.*, 647 (2011).
24. E. Lee, J. W. Cho, J. Kim, J. Yun, J. H. Kim and B. K. Min, *J. Alloy Compd.*, **506**, 969 (2010).
25. J. Olejnicek, C. A. Kamler, A. Mirasano, A. L. Martinez-Skinner, M. A. Ingersoll, C. L. Exstrom, S. A. Darveau, J. L. Huguenin-Love, M. Diaz, N. J. Ianno and R. J. Soukup, *Sol. Energy Mater. Sol. C*, **94**, 8 (2010).
26. B. Koo, R. N. Patel and B. A. Korgel, *J. American Chem. Soc.*, **131**, 3134 (2009).
27. Q. Guo, S. J. Kim, M. Kar, W. N. Shafarman, R. W. Birkmire, E. A. Stach, R. Agrawal and H. W. Hillhouse, *Nano Lett.*, **8**, 2982 (2008).
28. D. S. Wang, W. Zheng, C. H. Hao, Q. Peng and Y. D. Li, *Chem. Commun.*, 2556 (2008).
29. S. Ahn, K. Kim, Y. Chun and K. Yoon, *Thin Solid Films*, **515**, 4036 (2007).
30. H. Z. Zhong, Y. C. Li, M. F. Ye, Z. Z. Zhu, Y. Zhou, C. H. Yang and Y. F. Li, *Nanotechnology*, **18** (2007).
31. K. H. Kim, Y. G. Chun, B. O. Park and K. H. Yoon, *Mater. Sci. Forum.*, **449-4**, 273 (2004).
32. B. Li, Y. Xie, J. X. Huang and Y. T. Qian, *Adv. Mater.*, **11**, 1456 (1999).
33. S. H. Chang, M. Y. Chiang, C. C. Chiang, F. W. Yuan, C. Y. Chen, B. C. Chiu, T. L. Kao, C. H. Lai and H. Y. Tuan, *Energy Environ. Sci.*, **4**, 4929 (2011).
34. M. Law, *Abstr. Pap. Am. Chem. S*, **241** (2011).
35. M. G. Panthani, V. Akhavan, B. Goodfellow, J. P. Schmidtke, L. Dunn, A. Dodabalapur, P. F. Barbara and B. A. Korgel, *J. American Chem. Soc.*, **130**, 16770 (2008).
36. C. J. Stolle, T. B. Harvey and B. A. Korgel, *Current Opinion in Chemical Engineering*, **2**, 160 (2013).
37. C. H. Chang and J. M. Ting, *Thin Solid Films*, **517**, 4174 (2009).
38. C. D. Donega, P. Liljeroth and D. Vanmaekelbergh, *Small*, **1**, 1152 (2005).
39. C. B. Murray, C. R. Kagan and M. G. Bawendi, *Annu. Rev. Mater. Sci.*, **30**, 545 (2000).
40. F. Kessler and D. Rudmann, *Sol. Energy*, **77**, 685 (2004).
41. H. Zhong, Z. Wang, E. Bovero, Z. Lu, F. C. J. M. van Veggel and G. D. Scholes, *J. Phys. Chem. C*, **115**, 12396 (2011).
42. P. M. Allen and M. G. Bawendi, *J. American Chem. Soc.*, **130**, 9240 (2008).
43. R. I. Walton, *Chem. Soc. Rev.*, **31**, 230 (2002).
44. V. A. Akhavan, M. G. Panthani, B. W.; Goodfellow, D. K. Reid and B. A. Korgel, *Opt. Express*, **18**, A411 (2010).
45. V. A. Akhavan, B. W. Goodfellow, M. G. Panthani, D. K. Reid, D. J. Hellebusch, T. Adachi and B. A. Korgel, *Energy Environ. Sci.*, **3**, 1600 (2010).
46. Q. Guo, G. M. Ford, H. W. Hillhouse and R. Agrawal, *Nano Lett.*, **9**, 3060 (2009).
47. S. Ahn, K. Kim, A. Cho, J. Gwak, J. H. Yun, K. Shin, S. Ahn and K. Yoon, *Acs. Appl. Mater. Int.*, **4**, 1530 (2012).
48. S. Jeong, B. S. Lee, S. Ahn, K. Yoon, Y. H. Seo, Y. Choi and B. H. Ryu, *Energy Environ. Sci.*, **5**, 7539 (2012).

49. Q. J. Guo, G. M. Ford, R. Agrawal and H. W. Hillhouse, *Prog. Photovoltaics*, **21**, 64 (2013).
50. J. Hedstrom, H. Ohlsen, M. Bodegard, A. Klyner, L. Stolt, D. Hariskos, M. Ruckh and H.-W. Schock, Photovoltaic Specialists Conference, 364 (1993).
51. M. Bodeg Ård, K. Granath and L. Stolt, *Thin Solid Films*, **361-362**, 9 (2000).
52. D. Rudmann, G. Bilger, M. Kaelin, F. J. Haug, H. Zogg and A. N. Tiwari, *Thin Solid Films*, **431-432**, 37 (2003).
53. J. W. Park, Y. W. Choi, E. Lee, O. S. Joo, S. Yoon and B. K. Min, *J. Cryst. Growth*, **311**, 2621 (2009).
54. D. Lee, Y. Choi and K. Yong, *J. Cryst. Growth*, **312**, 3665 (2010).
55. L. Li, N. Coates and D. Moses, *J. American Chem. Soc.*, **132**, 22 (2010).
56. M. Kaelin, D. Rudmann, F. Kurdesau, H. Zogg, T. Meyer and A. N. Tiwari, *Thin Solid Films*, **480**, 486 (2005).
57. B. D. Weil, S. T. Connor and Y. Cui, *J. American Chem. Soc.*, **132**, 6642 (2010).
58. W. Wang, Y. W. Su and C. H. Chang, *Sol. Energy Mater. Sol. C*, **95**, 2616 (2011).
59. S. Ahn, T. H. Son, A. Cho, J. Gwak, J. H. Yun, K. Shin, S. K. Ahn, S. H. Park and K. Yoon, *Chemsuschem*, **5**, 1773 (2012).
60. A. R. Uhl, C. Fella, A. Chirila, M. R. Kaelin, L. Karvonen, A. Weidenkaff, C. N. Borca, D. Grolimund, Y. E. Romanyuk and A. N. Tiwari, *Prog. Photovoltaics*, **20**, 526 (2012).
61. G. Wang, S. Y. Wang, Y. Cui and D. C. Pan, *Chem. Mater.*, **24**, 3993 (2012).
62. W. Wang, S. Y. Han, S. J. Sung, D. H. Kim and C. H. Chang, *Phys. Chem. Chem. Phys.*, **14**, 11154 (2012).
63. S. J. Park, J. W. Cho, J. K. Lee, K. Shin, J.-H. Kim and B. K. Min, *Progress in Photovoltaics: Research and Applications*, n/a (2013).
64. W. Zhao, Y. Cui and D. Pan, *Energy Technol.*, **1**, 131 (2013).
65. D. B. Mitzi, M. Yuan, W. Liu, A. J. Kellock, S. J. Chey, V. Deline and A. G. Schrott, *Adv. Mater.*, **20**, 3657 (2008).
66. D. B. Mitzi, M. Yuan, W. Liu, A. J. Kellock, S. J. Chey, L. Gignac and A. G. Schrott, *Thin Solid Films*, **517**, 2158 (2009).
67. W. Liu, D. B. Mitzi, M. Yuan, A. J. Kellock, S. J. Chey and O. Gunawan, *Chem. Mater.*, **22**, 1010 (2010).
68. T. K. Todorov, O. Gunawan, T. Gokmen and D. B. Mitzi, *Prog. Photovoltaics*, **21**, 82 (2013).
69. D. B. Mitzi, L. L. Kosbar, C. E. Murray, M. Copel and A. Afzali, *Nature*, **428**, 299 (2004).
70. B. Bob, B. Lei, C. H. Chung, W. B. Yang, W. C. Hsu, H. S. Duan, W. W. J. Hou, S. H. Li and Y. Yang, *Adv. Energy Mater.*, **2**, 504 (2012).
71. T. P. Niesen and M. R. De Guire, *Solid State Ionics*, **151**, 61 (2002).
72. D. Lee and K. Yong, *Acs. Appl. Mater. Int.*, **4**, 6757 (2012).
73. S. Ahn, C. Kim, J. H. Yun, J. Gwak, S. Jeong, B. H. Ryu and K. Yoon, *J. Phys. Chem. C*, **114**, 8108 (2010).
74. V. Haug, A. Quintilla, I. Klugius and E. Ahlswede, *Thin Solid Films*, **519**, 7464 (2011).
75. M. Seol, H. Kim, Y. Tak and K. Yong, *Chem. Commun.*, **46**, 5521 (2010).
76. H. Kim, H. Jeong, T. K. An, C. E. Park and K. Yong, *Acs. Appl. Mater. Int.*, **5**, 268 (2012).
77. M. Seol, E. Ramasamy, J. Lee and K. Yong, *The J. Phys. Chem. C*, **115**, 22018 (2011).
78. I. Hwang and K. Yong, *Chem. Phys. Chem.*, **14**, 364 (2013).
79. J. W. Cho, S. J. Park, J. Kim, W. Kim, H. K. Park, Y. R. Do and B. K. Min, *Acs. Appl. Mater. Int.*, **4**, 849 (2012).
80. H. Kim and K. Yong, *Phys. Chem. Chem. Phys.*, **15**, 2109 (2013).
81. D. H. Youn, M. Seol, J. Y. Kim, J. W. Jang, Y. Choi, K. Yong and J. S. Lee, *Chemsuschem*, **6**, 261 (2013).
82. Y. Tak, S. J. Hong, J. S. Lee and K. Yong, *J. Mater. Chem.*, **19**, 5945 (2009).

Kijung Yong is a Professor in the Department of Chemical Engineering at POSTECH in Korea. He received his B.S. degree (Yonsei University, Korea), M.S. degree (Yonsei University, Korea), and Ph.D. degree (Carnegie Mellon University) all in Chemical Engineering and was a postdoctoral fellow at the University of Texas at Austin. He joined POSTECH in 1997. His research interests include nanomaterial synthesis/applications, solar energy conversion, biomimetics, and surface chemistry.